

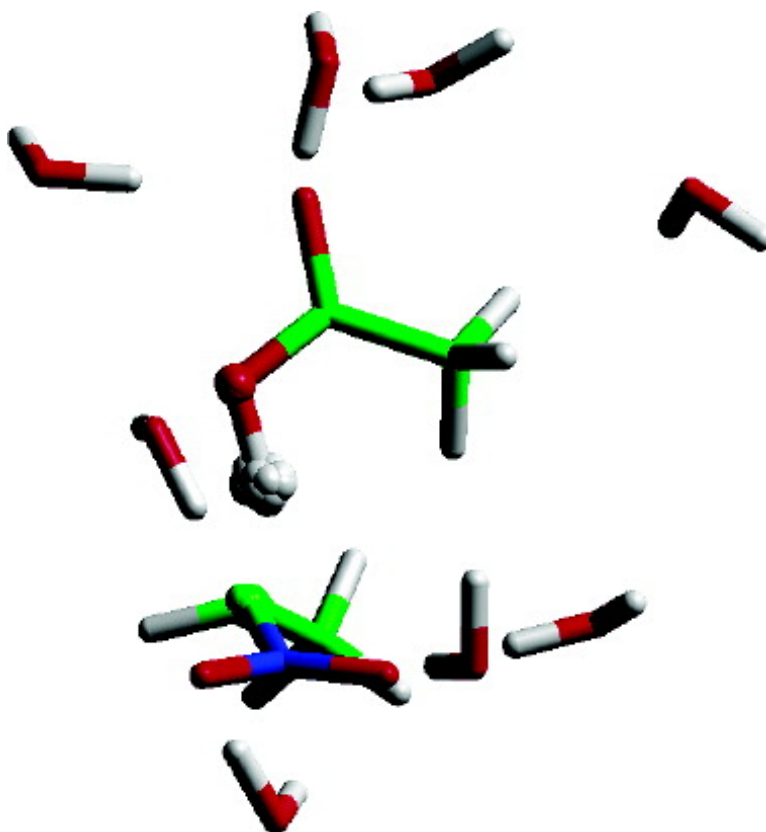
Communication

Solvent Polarization and Kinetic Isotope Effects in Nitroethane Deprotonation and Implications to the Nitroalkane Oxidase Reaction

Dan T. Major, Darrin M. York, and Jiali Gao

J. Am. Chem. Soc., **2005**, 127 (47), 16374-16375 • DOI: 10.1021/ja055881u • Publication Date (Web): 08 November 2005

Downloaded from <http://pubs.acs.org> on March 25, 2009



More About This Article

Additional resources and features associated with this article are available within the HTML version:

- Supporting Information
- Links to the 8 articles that cite this article, as of the time of this article download
- Access to high resolution figures



- Links to articles and content related to this article
- Copyright permission to reproduce figures and/or text from this article

[View the Full Text HTML](#)



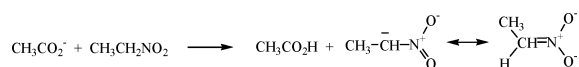
Solvent Polarization and Kinetic Isotope Effects in Nitroethane Deprotonation and Implications to the Nitroalkane Oxidase Reaction

Dan T. Major,* Darrin M. York, and Jiali Gao*

Department of Chemistry and Supercomputing Institute, Digital Technology Center, University of Minnesota, Minneapolis, Minnesota 55455

Received August 26, 2005; E-mail: major@chem.umn.edu; gao@chem.umn.edu

The unusual Brønsted relationship between rates and equilibria for deprotonation of nitroalkanes in water is known as the nitroalkane anomaly.¹ Further, protic solvation significantly increases the barrier height.^{1,2} Bernasconi rationalized this phenomenon based on the principle of nonperfect synchronization (PNS), which states that the rate constant is decreased when product stabilizing factors lag behind the transition state.² Computational studies^{3,4} in the gas phase showed that the anionic charge delocalization occurs later than proton abstraction, and nitroalkane ionization is predicted to have large solvent effects with increased free energy barrier in protic solvents.^{1,2}



The deprotonation of nitroalkanes is catalyzed by the flavoenzyme nitroalkane oxidase, in which the removal of the α -proton of nitroethane by Asp402 is rate-limiting. The second-order rate constant is enhanced by a factor of 10^9 over the uncatalyzed reaction in water,⁵ and the deuterium kinetic isotope effects (KIEs) were found to be 9.2 in the enzyme and 7.8 in water. The similarity in KIE has been described as evidence for lacking tunneling contributions to rate enhancement by the enzyme.⁵ Nevertheless, the large magnitude of the observed KIEs suggests that quantum effects can be important in determining the absolute rate constants. Here, we report a computational study that reveals the role of solvent polarization effects and quantum mechanical contributions in rate calculation.

We employ a mixed molecular dynamics and centroid path integral (CPI) simulation technique to describe the nuclear quantum effects and a combined quantum mechanical and molecular mechanical (QM/MM) method to represent the potential surface.⁷⁻⁹ In the CPI calculation, the QM contributions are incorporated into the classical potential of mean force (PMF) as a correction.⁸ In the present study, the centroid positions of the three quantized nuclei ($\text{C}_\alpha\text{-H}\cdots\text{O}$ atoms) are constrained to coincide with their atomic coordinates, and we used a bisection sampling procedure that improves the convergence of CPI results.⁷ For the QM/MM potential,⁹ we used the semiempirical Austin model 1 (AM1) Hamiltonian that was reparametrized to fit the energies for the reaction in the gas phase obtained experimentally or at the Gaussian3 (G3) theory. Consequently, the quality of such a reaction-specific (RS-AM1) model is comparable to ab initio calculations at the G3 level. We note that the calibration was done only for the reaction in the gas phase, that is, the intrinsic performance of the QM model. Solvent effects and nuclear quantum contributions are derived from subsequent molecular dynamics and CPI simulations.

The classical PMF was obtained from a series of 17 umbrella sampling simulations (windows) for a system consisting of the "QM reactants", nitroethane, and acetate ion, plus a sodium ion and 898

Table 1. Computed KIEs and Free Energies of Activation and Reaction (kcal/mol) for Nitroethane Deprotonation by Acetate Ion

	gas ^a		aqueous		exp
	CM	QM	CM	QM	
ΔG^\ddagger	11.7	9.2	28.9	25.9	24.8 ± 0.2
ΔG_{rxn}	7.5	7.6	5.4	5.6	5.2
KIE ^b		5.0 (4.6)		6.0 (5.4)	7.8 ± 0.1

^a Computed using the RS-AM1 model. For comparison, the energies of reaction are 9.8 and -9.5 kcal/mol from ab initio G3 and AM1 calculations.
^b Total KIEs are given, and primary KIEs are in parentheses. Secondary KIEs are 1.09 and 1.10 in the gas phase and in water, respectively.

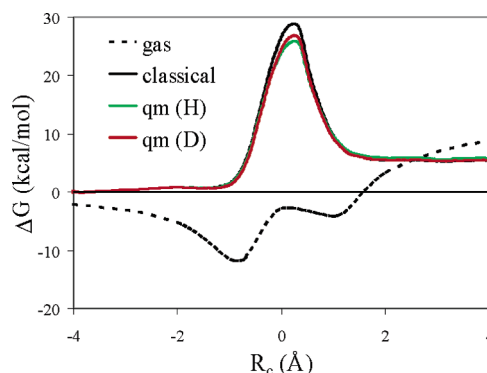


Figure 1. Computed potential of mean force for the proton and deuteron abstraction of nitroethane by acetate ion in water. The reaction coordinate is defined as the difference of the distances of the α -proton (or deuterium) from the C_α atom and the acetate oxygen, $R_c = R(\text{C-H}) - R(\text{H-O})$.

water molecules in a box of ca. $30 \times 30 \times 30 \text{ \AA}^3$. This gives the classical (CM) free energy of activation ΔG^\ddagger in Table 1. Periodic boundary conditions were used along with the particle mesh-Ewald method to treat long-range electrostatic effects for QM/MM simulations.¹⁰ Each simulation window includes at least 100 ps of equilibration followed by 100 ps of averaging at 25 °C. The quantum mechanical PMF was obtained by CPI calculations on configurations from umbrella sampling simulations.^{7,8} Each quantized particle was represented by 32 beads, and convergence was validated by using 8, 16, and 64 beads. A total of 10^5 free-particle configurations were sampled in the CPI simulation.

Key results are shown in Figure 1, which displays the classical and quantum mechanical PMF for the proton (deuteron) abstraction of nitroethane by an acetate ion. First, solvent effects are significant on the proton abstraction reaction. In the gas phase, the free energy barrier ΔG^\ddagger is 9.2 kcal/mol from the ion-dipole complex, which is increased to 25.9 kcal/mol in water (Table 1). Second, solvation effects are less pronounced on the equilibrium constant, lowering ΔG_{rxn} by only 2 kcal/mol. Both computed ΔG^\ddagger and ΔG_{rxn} are in accord with experiments.^{1,5,11} Finally, nuclear quantum effects (zero-point and tunneling) are critical to computation of the rate constant. Inclusion of these effects lowers the classical barrier by 3.0 (2.0)

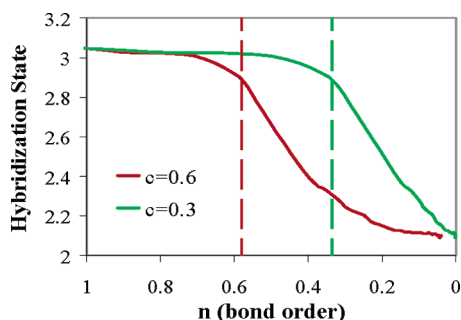


Figure 2. Hybridization state of the C_{α} atom as a function of the Pauling bond order for the breaking C_{α} –H bond as an indicator of reaction progress; $n = n_0 \exp[(r_0 - r_{C-H})/c]$, where $c = 0.3$ for standard bonds and 0.6 for transition structures. The location of the TS is specified by the vertical lines for different c values. The C_{α} –H bond order changes from one to zero in the reaction as the C_{α} atom changes from an sp^3 to an sp^2 hybridization.

kcal/mol for proton (deuterium) abstraction. In all, the computed KIE is 5.4 for a singly deuterated nitroethane, and the total KIE is increased to 6.0 for $[1,1\text{-}^2\text{H}_2]$ nitroethane. This may be compared with the corresponding experimental value of 7.8.⁵ Importantly, these agreements with experiment justify further analyses of the results to gain insight into the origin of solvation and quantum effects.

The high barrier to proton transfer in water is due to preferential solvation of the reactant and product state.² In the reactant state, the carboxylate group is strongly stabilized by water (-80 kcal/mol).¹³ For the product, the carbanion is best represented by a resonance structure that has the anionic charge delocalized on the nitro group, which is also well stabilized, as indicated by the modest solvent effects on equilibrium ΔG_{rxn} (Table 1). However, at the transition state (TS), the anionic charge is spread in both the substrate and nucleophile, resulting in poorer solvation in comparison with the reactant state. To provide insight into the unusually large solvent effects on ΔG^{\ddagger} , we analyzed the solute–solvent (QM/MM) interaction energies using a decomposition method described in ref 13. Specifically, we obtained average solute–solvent polarization energies of -8.3 , -7.4 , and -28 kcal/mol for the reactants, TS, and products, respectively, revealing that solvent polarization energy is a major factor in product stabilization. The small solvent polarization stabilization at the TS is due to slow structural changes at the C_{α} center, which lags behind the progress of the reaction coordinate. Figure 2 depicts the change of the C_{α} rehybridization as a function of the C_{α} –H bond order, n , along the reaction path. At the TS, the C_{α} –H bond breaking process ($n = 0.4\text{--}0.6$) is half complete; however, little rehybridization has occurred at the C_{α} center, preventing effective charge delocalization into the nitro group. A favorable charge transfer would have resulted in greater solvent stabilization, thereby smaller solvent effects. This is consistent with the conclusion based on the PNS; here, we have identified that the consequence of the structural changes is a smaller solvent polarization interaction energy at the transition state.

We have addressed the question of differential nuclear QM effects in the gas phase and in solution. The computed KIEs are similar for the reaction in the two phases. For proton abstraction, the total quantum effects lower the classical ΔG^{\ddagger} by 2.5 kcal/mol in the gas phase, compared to 3.0 kcal/mol in water. To separate tunneling and bound vibrations, we used the ensemble-averaged variational transition state theory with multidimensional tunneling to obtain the tunneling transmission coefficient κ .¹⁴ In the gas phase, there is little tunneling ($\kappa \approx 1$), whereas solvation induces a small, but noticeable tunneling contribution in water ($\langle \kappa \rangle = 1.5$). Further, tunneling has a relatively small effect on the computed KIEs both in the gas phase and in water, consistent with the conclusions in

ref 5. The small difference in the computed KIEs in the gas phase and water can also be attributed to bound vibrations due to the change in the transition state geometry, which is located at 0.10 Å in the gas phase and 0.27 Å in water. The latter corresponds to a more loose TS, resulting in greater changes in quantum vibrational energy.

In summary, our results show that the difference in solvent polarization effects for the TS and products is a major factor for the differential solvent effects on rate and equilibrium of nitroalkane deprotonation. This is due to high charge density at C_{α} and poor charge delocalization in the TS as a result of slower rehybridization than the progress of the reaction coordinate. This is consistent with the qualitative picture from the PNS.² Solvent effects only enhance the computed kinetic isotope effects by 20% in comparison with the gas-phase value, which may be attributed to the slight solvent-induced increase in tunneling and zero-point effects. The present results suggest that an effective means by which the transition state can be stabilized in the enzyme is to facilitate the C_{α} rehybridization by specific hydrogen bonding interactions, or by desolvation in view of the large solvent effects on the reaction barrier in water.¹⁵ It will be of great interest to examine these hypotheses for the reaction in nitroalkane oxidase.⁶

Acknowledgment. This work has been supported by the National Institutes of Health, and D.T.M. is a Fulbright Scholar.

Supporting Information Available: Optimized reaction-specific AM1 (RS-AM1) parameters (6 pages, print/PDF). This material is available free of charge via the Internet at <http://pubs.acs.org>.

References

- (1) (a) Kresge, A. *Can. J. Chem.* **1974**, *52*, 1897. (b) Bordwell, F. G.; Boyle, W. J., Jr. *J. Am. Chem. Soc.* **1972**, *94*, 3907. (c) Keeffe, J. R.; Morey, J.; Palmer, C. A.; Lee, J. C. *J. Am. Chem. Soc.* **1979**, *101*, 1295.
- (2) (a) Bernasconi, C. F. *Acc. Chem. Res.* **1992**, *25*, 9. (b) Bernasconi, C. F. *Adv. Phys. Org. Chem.* **1992**, *27*, 119. (c) Bernasconi, C. F.; Wenzel, P. *J. Am. Chem. Soc.* **1994**, *116*, 5405.
- (3) (a) Keeffe, J. R.; Gronert, S.; Colvin, M. E.; Tran, N. L. *J. Am. Chem. Soc.* **2003**, *125*, 11730. (b) Richard, J. P.; Williams, G.; Gao, J. *J. Am. Chem. Soc.* **1999**, *121*, 715.
- (4) (a) Yamataka, H.; Mishima, M. *J. Am. Chem. Soc.* **1999**, *121*, 10223. (b) Beksic, D.; Bertran, J.; Lluch, J. M.; Hynes, J. T. *J. Phys. Chem. A* **1998**, *102*, 3977. (c) Pross, A.; Shaik, S. S. *J. Am. Chem. Soc.* **1982**, *104*, 1129. (d) Costentin, C.; Saveant, J.-M. *J. Am. Chem. Soc.* **2004**, *126*, 14787.
- (5) (a) Valley, M. P.; Fitzpatrick, P. F. *J. Am. Chem. Soc.* **2004**, *126*, 6244. (b) Valley, M. P.; Fitzpatrick, P. F. *Biochemistry* **2003**, *42*, 5850. (c) Valley, M. P.; Tichy, S. E.; Fitzpatrick, P. F. *J. Am. Chem. Soc.* **2005**, *127*, 2062.
- (6) Nagpal, A.; Valley, M. P.; Fitzpatrick, P. F.; Orville, A. M. *Acta Crystallogr.* **2004**, *D60*, 1456.
- (7) Major, D. T.; Gao, J. *J. Mol. Graph. Modeling* **2005**, *24*, 121.
- (8) Hwang, J.-K.; Chu, Z. T.; Yadav, A.; Warshel, A. *J. Phys. Chem.* **1991**, *95*, 8445.
- (9) (a) Gao, J. *Rev. Comput. Chem.* **1995**, *7*, 119. (b) Field, M. J.; Bash, P. A.; Karplus, M. *J. Comput. Chem.* **1990**, *11*, 700.
- (10) Nam, K.; Gao, J.; York, D. M. *J. Chem. Theor. Comput.* **2005**, *1*, 2.
- (11) (a) Jencks, W. P.; Regenstein, J. In *Handbook of Biochemistry and Molecular Biology*; Fassman, G., Ed.; Chemical Rubber Company: Cleveland, OH, 1976; Vol. 1, p 305. (b) Kresge, A. J.; Drake, D. A.; Chiang, Y. *Can. J. Chem.* **1974**, *52*, 1889. (c) Pearson, R. G.; Dillon, R. L. *J. Am. Chem. Soc.* **1953**, *75*, 2439.
- (12) Pu, J.; Ma, S.; Garcia-Viloca, M.; Gao, J.; Truhlar, D. G. *J. Am. Chem. Soc.* **2005**, *127*, 14879.
- (13) (a) Gao, J.; Xia, X. *Science* **1992**, *258*, 631. The polarization energy is defined as $\Delta E_{\text{pol}} = \langle \Psi_{\text{aq}} | H^{\circ} + H_{\text{qm}/\text{mm}} | \Psi_{\text{aq}} \rangle - \langle \Psi^{\circ} | H^{\circ} | \Psi^{\circ} \rangle$, where Ψ_{aq} and Ψ° are the solute wave functions in water and in the gas phase that optimize the Hamiltonians $H^{\circ} + H_{\text{qm}/\text{mm}}$ and H° with H° being in the gas phase and $H_{\text{qm}/\text{mm}}$ representing solute–solvent interactions. See also: (b) Garcia-Viloca, M.; Gao, J.; Truhlar, D. G. *J. Mol. Biol.* **2003**, *327*, 549.
- (14) Alhambra, C.; Corchado, J. C.; Sanchez, M. L.; Garcia-Viloca, M.; Gao, J.; Truhlar, D. G. *J. Phys. Chem. B* **2001**, *105*, 11326.
- (15) (a) Gerlt, J. A.; Gassman, P. G. *J. Am. Chem. Soc.* **1993**, *115*, 11552. (b) Nam, K.; Prat-Resina, X.; Garcia-Viloca, M.; Devi-Kesavan, L. S.; Gao, J. *J. Am. Chem. Soc.* **2004**, *126*, 1369.

JA055881U